Molecular Physics
Vol. 106, Nos. 2–4, 2008, 397–404

RESEARCH ARTICLE

Inelastic effects in molecular junction transport: scattering and self-consistent calculations for the Seebeck coefficient

Michael Galperin[a], Abraham Nitzan[b*] and Mark A. Ratner[a]

[a]*Department of Chemistry and Materials Research Center, Northwestern University, Evanston, IL 60208, USA;* [b]*School of Chemistry, The Sackler Faculty of Science, Tel Aviv University, Tel Aviv 69978, Israel*

(*Received 22 September 2007; final version recevied 29 November 2007*)

The influence of molecular vibration on the Seebeck coefficient is studied within a simple model. Results of a scattering theory approach are compared with those of a full self-consistent non-equilibrium Green's function scheme. We show, for a reasonable choice of parameters, that inelastic effects have a non-negligible influence on the resulting Seebeck coefficient for the junction. We note that the scattering theory approach may fail both quantitatively and qualitatively. The results of calculations with reasonable parameters are in good agreement with recent measurements [Science **315**, 1568 (2007)].

Keywords: molecular junctions; Seebeck coefficient; thermoelectricity; electron–phonon interaction; inelastic effects

1. Introduction

The development of experimental techniques for constructing and exploring molecular devices has inspired extensive theoretical study of charge transport in molecules, with potential application in molecular electronics [1–4]. One important issue related to the stability of potential molecular devices involves heating and heat transport in molecular junctions. This topic has attracted attention both experimentally [5–10] and theoretically [11–21]. Another closely related issue involves the thermoelectric properties of such devices. While thermoelectricity in the bulk is well studied, corresponding measurements in molecular junctions were reported only recently [22,23].

Electron–vibration interactions in the junction (leading to inelastic effects in charge transport [24]) may cause junction heating and affect its heat transport properties [21]. Theoretical considerations of thermoelectric properties so far either completely disregard such effects (in treatments based on the Landauer theory [23,25,26]) or include it within a scattering theory framework [27,28]. The latter treats the effect of vibrations as an inelastic electron scattering process, and changes in the non-equilibrium distributions of electrons and vibrations are not described in a self-consistent manner. It has been shown that such changes may have qualitative effects on the transport [29,30]. Note also that scattering theory approaches may lead to erroneous predictions due to the neglect of the effects of the contacts' Fermi seas on the junction electronic structure [31].

This paper was motivated by recent measurements of the Seebeck coefficient in molecular junctions [23]. Considerations based on the Landauer formula were employed there to interpret the experimental data. Our goals here are: (1) to show the importance of vibrations for the Seebeck coefficient; and (2) to include vibrations in a fully self-consistent way within the non-equilibrium Green's function approach for calculating the Seebeck coefficient.

The structure of the paper is as follows. Section 2 introduces the model, discusses the methods used in the calculations, and presents a simple (approximate) analytical derivation to illustrate the change in the Seebeck coefficient expression (as compared with the Landauer-based expression) when vibrations are taken into account. Section 4 presents the numerical results obtained in a fully self-consistent way.

2. Model

We consider a simple resonant-level model with the electronic level $|0\rangle$ coupled to two electrodes left (L) and right (R) (each a free electron reservoir at its

Corresponding author: Email: nitzan@post.tau.ac.il

ISSN 0026–8976 print/ISSN 1362–3028 online

DOI: 10.1080/00268970701837784
http://www.informaworld.com

own equilibrium). The electron on the resonant level (electronic energy ε_0) is linearly coupled to a single vibrational mode (referred to below as the primary phonon) with frequency ω_0. The latter is coupled to a phonon bath represented as a set of independent harmonic oscillators (secondary phonons). The system Hamiltonian is (here and below we use $\hbar = 1$ and $e = 1$)

$$\hat{H} = \varepsilon_0 \hat{c}^\dagger \hat{c} + \sum_{k\in\{L,R\}} \varepsilon_k \hat{c}_k^\dagger \hat{c}_k + \sum_{k\in\{L,R\}} (V_k \hat{c}_k^\dagger \hat{c} + h.c.) + \omega_0 \hat{a}^\dagger \hat{a} + \sum_\beta \omega_\beta \hat{b}_\beta^\dagger \hat{b}_\beta + M_a \hat{Q}_a \hat{c}^\dagger \hat{c} + \sum_\beta U_\beta \hat{Q}_a \hat{Q}_\beta, \tag{1}$$

where $\hat{c}^\dagger$ ($\hat{c}$) are creation (destruction) operators for electrons on the bridge level, $\hat{c}_k^\dagger$ ($\hat{c}_k$) are the corresponding operators for electronic states in the contacts, $\hat{a}^\dagger$ ($\hat{a}$) are creation (destruction) operators for the primary phonon, and $\hat{b}_\beta^\dagger$ ($\hat{b}_\beta$) are the corresponding operators for phonon states in the thermal (phonon) bath. $\hat{Q}_a$ and $\hat{Q}_\beta$ are phonon displacement operators

$$\hat{Q}_a = \hat{a} + \hat{a}^\dagger, \qquad \hat{Q}_\beta = \hat{b}_\beta + \hat{b}_\beta^\dagger. \tag{2}$$

The energy parameters M_a and U_β correspond to the vibronic and the vibrational coupling, respectively. Equation (1) is often used as a generic model for describing the effects of vibrational motion on electronic conduction in molecular junctions [24].

After a small polaron (canonical or Lang–Firsov) transformation [32,33] the Hamiltonian (1) takes the form [29]

$$\hat{\bar{H}} = \bar{\varepsilon}_0 \hat{c}^\dagger \hat{c} + \sum_{k\in\{L,R\}} \varepsilon_k \hat{c}_k^\dagger \hat{c}_k + \sum_{k\in\{L,R\}} (V_k \hat{c}_k^\dagger \hat{c} \hat{X}_a + \text{h.c.}) + \omega_0 \hat{a}^\dagger \hat{a} + \sum_\beta \omega_\beta \hat{b}_\beta^\dagger \hat{b}_\beta + \sum_\beta U_\beta \hat{Q}_a \hat{Q}_\beta, \tag{3}$$

where

$$\bar{\varepsilon}_0 = \varepsilon_0 - \Delta, \quad \Delta \approx \frac{M_a^2}{\omega_0}, \tag{4}$$

$$\hat{X}_a = \exp[i\lambda_a \hat{P}_a], \quad \lambda_a = \frac{M_a}{\omega_0}. \tag{5}$$

Δ is the electron level shift due to coupling to the primary phonon and $\hat{X}_a$ is the primary phonon shift generator. $\hat{P}_a = -i(\hat{a} - \hat{a}^\dagger)$ is the phonon momentum operator.

The mathematical quantity of interest is the single electron Green function (GF) on the Keldysh contour

$$G(\tau_1, \tau_2) \equiv -i\langle T_c \hat{c}(\tau_1) \hat{c}^\dagger(\tau_2)\rangle_H. \tag{6}$$

We approximate it by [29]

$$G(\tau_1, \tau_2) \approx -\frac{i}{\hbar}\langle T_c \hat{c}(\tau_1)\hat{c}^\dagger(\tau_2)\rangle_{\bar{H}} \times \langle \hat{X}_a(\tau_1)\hat{X}_a^\dagger(\tau_2)\rangle_{\bar{H}} \equiv G_c(\tau_1, \tau_2)\mathcal{K}(\tau_1, \tau_2), \tag{7}$$

where $G_c(\tau_1, \tau_2)$ is the pure electronic GF and $\mathcal{K}(\tau_1, \tau_2)$ corresponds to the Franck–Condon factor. We have developed [29] a self-consistent scheme for evaluating this function, leading to the coupled set of equations

$$\mathcal{K}(\tau_1, \tau_2) = \exp\{\lambda_a^2[iD_{P_aP_a}(\tau_1, \tau_2) - \langle \hat{P}_a^2\rangle]\}, \tag{8}$$

$$D_{P_aP_a}(\tau, \tau') = D^{(0)}_{P_aP_a}(\tau, \tau') + \int_c d\tau_1 \int_c d\tau_2 D^{(0)}_{P_aP_a}(\tau, \tau_1) \times \Pi_{P_aP_a}(\tau_1, \tau_2) D_{P_aP_a}(\tau_2, \tau'), \tag{9}$$

$$G_c(\tau, \tau') = G_c^{(0)}(\tau, \tau') + \sum_{K=\{L,R\}} \int_c d\tau_1 \int_c d\tau_2 G_c^{(0)}(\tau, \tau_1) \times \Sigma_{c,K}(\tau_1, \tau_2) G_c(\tau_2, \tau'), \tag{10}$$

where $D_{P_aP_a}(\tau, \tau') \equiv -i\langle T_c \hat{P}_a(\tau)\hat{P}_a(\tau')\rangle$ is the phonon GF, and $D^{(0)}_{P_aP_a}$ and $G_c^{(0)}$ are the phonon and electron Green functions when the two sub-systems are uncoupled ($M_a = 0$). The functions $\Pi_{P_aP_a}$ and $\Sigma_{c,K}$ in Equations (9) and (10) are given by

$$\Pi_{P_aP_a}(\tau_1, \tau_2) = \sum_\beta |U_\beta|^2 D_{P_\beta P_\beta}(\tau_1, \tau_2) - i\lambda_a^2 \times \sum_{k\in\{L,R\}} |V_k|^2 [\hbar g_k(\tau_2, \tau_1) G_c(\tau_1, \tau_2) \mathcal{K}(\tau_1, \tau_2) + (\tau_1 \leftrightarrow \tau_2)], \tag{11}$$

$$\Sigma_{c,K}(\tau_1, \tau_2) = \sum_{k\in K} |V_k|^2 g_k(\tau_1, \tau_2)\langle T_c \hat{X}_a(\tau_2)\hat{X}_a^\dagger(\tau_1)\rangle. \tag{12}$$

Here, these functions play a role similar to self-energies in standard many-particle theory. Here, $K = L, R$ and g_k is the free electron Green function for state k in the contacts. Details of the derivation have been published by Galperin *et al.* [29]. A self-consistent solution scheme implies solving Equations (8)–(12) iteratively until convergence. As a convergence parameter we used the population of the level $n_0 = \langle \hat{c}^\dagger \hat{c}\rangle$. When n_0 for subsequent steps of the iterative cycle differed by less than a predefined tolerance (taken in the calculations below to be 10^{-6}), convergence was assumed to be achieved.

Once the electron GF (7) is obtained, its lesser and greater projections are used to obtain the steady-state current through the junction [34,35],

$$I_K = \langle \hat{I}_K\rangle = \int \frac{dE}{2\pi} [\Sigma_K^<(E) G^>(E) - \Sigma_K^>(E)\, G^<(E)], \tag{13}$$

at interface $K = L, R$. Here,

$$\Sigma_K^<(E) = if_K(E)\Gamma_K(E), \tag{14}$$
$$\Sigma_K^>(E) = -i[1 - f_K(E)]\Gamma_K(E), \tag{15}$$

with $f_K(E) = [\exp(\beta(E - \mu_K)) + 1]^{-1}$ being the Fermi distribution in the contact $K = L, R$ and

$$\Gamma_K(E) = 2\pi \sum_{k \in K} |V_k|^2 \delta(E - \varepsilon_k). \tag{16}$$

The Seebeck coefficient is defined by

$$S(I) = \frac{V(I)}{\Delta T(I)}, \tag{17}$$

where $V(I)$ is the voltage bias that yields current I at $\Delta T = 0$, and $\Delta T(I)$ is the temperature difference between the contacts that yields the same current at $V = 0$. The linear regime corresponds to the $I \to 0$ limit of Equation (17).

Below we present calculations of the Seebeck coefficient using different levels of approximation. In particular, we compare the results of a simple scattering theory-like approach and a full self-consistent calculation based on the procedure described above. The simple approach is essentially a first step of the full self-consistent iterative solution with the additional assumption of no coupling to the thermal bath for the molecular vibration ($U_\beta \to 0$ in Equation (3)).

Generally speaking, both the self-consistent and the scattering theory-like approaches are approximate, and more sophisticated schemes will be developed in the future to deal with electron–phonon interaction in transport. Note, however, that for simple model used (single level coupled to single vibration), the approach employed is essentially exact from the single-electron tunneling (i.e. scattering theory) point of view, since the canonical transformation solves exactly the electron–phonon coupling problem in the case of an isolated molecule. Note also that the main drawback of all scattering theory approaches is the fact that they disregard Fermi populations in the contacts. These populations have the effect of blocking one channel and distorting others, as was first reported by Mitra *et al.* [31]. It is this issue that leads to the (sometimes qualitative) failure of the scattering-theory-based results for transport, as is shown below, and is also true for the case of the Seebeck coefficient. Detailed discussions of different approximation schemes have been published by Galperin *et al.* [24].

3. Transport coefficients

Before presenting the results of the numerical calculations, we describe how the transport coefficients are introduced. In the Landauer regime of transport (electron–phonon interaction disregarded, both carriers scatter ballistically), the electric and thermal fluxes, I and J, are given by [21,25,36]

$$I = \frac{2|e|}{\hbar} \int_{-\infty}^{+\infty} \frac{\mathrm{d}E}{2\pi} \mathcal{T}_{\mathrm{el},0}(E)[f_L(E) - f_R(E)],$$
$$J = \frac{2}{\hbar} \int_{-\infty}^{+\infty} \frac{\mathrm{d}E}{2\pi} (E - E_\mathrm{F}) \mathcal{T}_{\mathrm{el},0}(E)[f_L(E) - f_R(E)]$$
$$+ \frac{1}{\hbar} \int_0^{\infty} \frac{\mathrm{d}\omega}{2\pi} \omega \mathcal{T}_{\mathrm{ph},0}(\omega)[N_L(\omega) - N_R(\omega)], \tag{18}$$

where E_F is a common Fermi energy in the absence of bias,

$$\mathcal{T}_{\mathrm{el},0}(E) = \mathrm{Tr}[\Gamma_L(E) G^r(E) \Gamma_R(E) G^a(E)],$$
$$\mathcal{T}_{\mathrm{ph},0}(\omega) = \mathrm{Tr}[\Omega_L(\omega) D^r(\omega) \Omega_R(\omega) D^a(\omega)] \tag{19}$$

are the electron and phonon transmission coefficients in the absence of electron–phonon coupling, and where

$$\Omega_K^{\mathrm{ph}}(\omega) \equiv 2\pi \sum_{\beta \in K} |U_\beta|^2 \delta(\omega - \omega_\beta), \quad K = L, R \tag{20}$$

is the broadening of the molecular vibration due to coupling to its thermal environment. In the linear response regime, the currents are linear in the applied driving forces – the bias V and the temperature difference ΔT,

$$I = G \cdot V + L \cdot \Delta T,$$
$$J = R \cdot V + F \cdot \Delta T. \tag{21}$$

Here, G and F are the electrical and thermal conduction, respectively, and L is known as the thermoelectric coefficient. The coefficients are given by [25,36]

$$G = -\frac{e^2}{\pi\hbar} \int_{-\infty}^{+\infty} \mathrm{d}E\, [-\beta f'(E)] \mathcal{T}_{\mathrm{el},0}(E), \tag{22}$$
$$L = -\frac{|e|}{\pi\hbar} \int_{-\infty}^{+\infty} \mathrm{d}E\, [-\beta f'(E)] \mathcal{T}_{\mathrm{el},0}(E) \frac{E - E_\mathrm{F}}{T}, \tag{23}$$
$$R = -\frac{|e|}{\pi\hbar} \int_{-\infty}^{+\infty} \mathrm{d}E\, [-\beta f'(E)] \mathcal{T}_{\mathrm{el},0}(E)$$
$$\times (E - E_\mathrm{F}) = L \cdot T, \tag{24}$$
$$F = \frac{1}{\pi\hbar} \int_{-\infty}^{+\infty} \mathrm{d}E\, [-\beta f'(E)] \mathcal{T}_{\mathrm{el},0}(E) \frac{(E - E_\mathrm{F})^2}{T}$$
$$+ \frac{1}{2\pi\hbar} \int_0^{\infty} \mathrm{d}\omega\, [-\beta N'(E)] \mathcal{T}_{\mathrm{ph},0}(\omega) \frac{\omega^2}{T}, \tag{25}$$

where $f'(E)$ is the derivative of the Fermi–Dirac distribution, $N'(\omega)$ is the derivative of the Bose–Einstein distribution, T is the temperature ($\beta = 1/T$), and E_F is the Fermi energy in the leads. Note the existence of the Onsager relation, $L \cdot T = R$, between the cross coefficients. Note also that the coefficient F in (25) contains two contributions, one corresponding to energy transfer by electrons, and the other to that by phonons. A discussion of the additive form of F and the relative importance of these contributions has been published by Galperin *et al*. [21]. The Seebeck coefficient is given in terms of these transport coefficients by

$$S = \frac{L}{G}. \tag{26}$$

Below we focus on these two coefficients – G and L – only. Making the approximation $[-\beta f'(E)] \approx \delta(E - E_F)$ in (22), and utilising the Sommerfield expansion [37] in (23), Equation (26) leads to

$$S = \frac{\pi^2 k_b^2 T}{3|e|} \frac{\partial \ln \mathcal{T}_{el,0}(E)}{\partial E}, \tag{27}$$

which is Equation (4) of Paulsson and Datta [25].

4. Calculation of the Seebeck coefficient

As discussed in Section 2, the simplest calculation that takes into account the electron–vibration interaction term (the M_a term in Equation (1)) corresponds to inelastic scattering of the transmitted electron from the phonon at the given initial temperature. Within the self-consistent scheme presented in Section 2 this result is obtained after the first iteration step, where the influence of the (free) vibration on the electronic GF is taken into account, but not *vice versa*. For this reason the coupling U_β to the thermal bath can be disregarded. For model (3) this calculation yields[†]

$$\begin{aligned} I = \frac{|e|}{\pi\hbar} \sum_{n,m=-\infty}^{+\infty} & I_n(2\lambda^2\sqrt{N_0(N_0+1)}) I_m(2\lambda^2\sqrt{N_0(N_0+1)}) \\ & \times e^{\beta(n+m)\omega_0/2 - 2\lambda^2(2N_0+1)} \int_{-\infty}^{+\infty} \mathrm{d}E\, \mathcal{T}_{el,0}(E) \\ & \times \{f_L(E+n\omega_0)[1-f_R(E-m\omega_0)] \\ & - f_R(E+m\omega_0)[1-f_L(E-n\omega_0)]\}, \end{aligned} \tag{28}$$

where $N_0 = [e^{\beta\omega_0} - 1]^{-1}$ and I_n is the modified Bessel function of order n [38]. For $M_a = 0$, Equation (28) reduces back to (18). Linearisation in the bias potential $V = V_L - V_R$ and in the temperature difference $\Delta T = T_L - T_R$ leads to the phonon-renormalised transport coefficients

$$\begin{aligned} G = -\frac{e^2}{\pi\hbar} \sum_{n,m=-\infty}^{+\infty} & I_n(2\lambda^2\sqrt{N_0(N_0+1)}) I_m(2\lambda^2\sqrt{N_0(N_0+1)}) \\ & \times e^{\beta(n+m)\omega_0/2 - 2\lambda^2(2N_0+1)} \int_{-\infty}^{+\infty} \mathrm{d}E \mathcal{T}_{el,0}(E) \\ & \times \{[-\beta f'(E-m\omega_0)] f(E+n\omega_0) \\ & + [-\beta f'(E+m\omega_0)][1-f(E-n\omega_0)]\}, \end{aligned} \tag{29}$$

$$\begin{aligned} L = -\frac{|e|}{\pi\hbar} \sum_{n,m=-\infty}^{+\infty} & I_n(2\lambda^2\sqrt{N_0(N_0+1)}) I_m(2\lambda^2\sqrt{N_0(N_0+1)}) \\ & \times e^{\beta(n+m)\omega_0/2 - 2\lambda^2(2N_0+1)} \int_{-\infty}^{+\infty} \mathrm{d}E\, \mathcal{T}_{el,0}(E) \\ & \times \left\{ [-\beta f'(E-m\omega_0)] f(E+n\omega_0) \frac{E-m\omega_0-E_F}{T} \right. \\ & + [-\beta f'(E+m\omega_0)][1-f(E-n\omega_0)] \\ & \left. \times \frac{E+m\omega_0-E_F}{T} \right\}. \end{aligned} \tag{30}$$

Using Equations (29) and (30), the Seebeck coefficient is calculated from Equation (26). To this end we first calculate the currents $I(V, \Delta T = 0)$ and $I(V = 0, \Delta T)$ as functions of V and ΔT. The inverted functions $V(I, \Delta T = 0)$ and $\Delta T(I, V = 0)$ are then used in (17) to

[†]To obtain Equation (28) from Equation (13) the 'first iterative step' of the self-consistent procedure [29] has to be taken. This leads to (see Equation (7))

$$G^{>,<}(t) = G_c^{>,<},(t)\mathcal{K}^{>,<}.$$

In order to keep the $L \leftrightarrow R$ symmetry for the current expression, one has to introduce the second FC factor in the Keldysh equation for G_c

$$G_c^{>,<}(t) = \sum_{K=L,R} \int_{-\infty}^{+\infty} \mathrm{d}t_1 \int_{-\infty}^{+\infty} \mathrm{d}t_2 G_c^r(t-t_1)\Sigma_K^{>,<}(t_1-t_2)\mathcal{K}^{<,>}(t_2-t_1)G^a(t_2).$$

Subsitituing these expreeesions into Equation (13) and expanding the FC factors in term of Bessel functions leads to Equation (28).

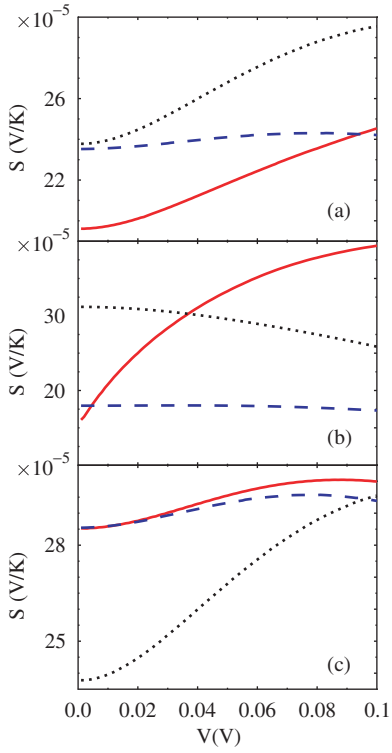

Figure 1. Seebeck coefficient versus applied bias. Shown are the results of the full self-consistent calculation (solid line, red), the scattering theory approach based on model (28) (dashed line, blue), and the elastic scattering case (dotted line, black) calculated using (a) the 'standard' set of parameters (see text for parameters), (b) a smaller $\varepsilon_0 - E_F$ gap, and (c) a weaker electron–phonon coupling M_a.

yield $S(I)$ (expressed below as $S(V)$ with $V = V(I, \Delta T = 0)$). In the calculations presented below, we have used symmetric bias and temperature differences across the junction: $\mu_{L,R} = E_F \pm V/2$, $T_{L,R} = T \pm \Delta T/2$.

Figure 1(a) shows the Seebeck coefficient S as a function of the bias potential, calculated at $T = 300\,\mathrm{K}$ using the energetic parameters $E_F = 0$, $\varepsilon_0 = 0.2\,\mathrm{eV}$, $\Gamma_L = \Gamma_R = 0.005\,\mathrm{eV}$, $\omega_0 = 0.05\,\mathrm{eV}$, $M_a = 0.1\,\mathrm{eV}$, and $\Omega_L^{\mathrm{ph}} = \Omega_R^{\mathrm{ph}} = 0.005\,\mathrm{eV}$. The latter is a wide-band approximation for molecular vibration broadening (20) due to coupling to thermal baths (for a detailed discussion, see the report of Galperin *et al.* [39]. Figure 1(b) and (c) show similar results for a smaller $\varepsilon_0 - E_F$ gap and a weaker electron–phonon coupling M_a, respectively. To show the effect of electron–phonon coupling on the Seebeck coefficient we compare the results obtained from the full self-consistent calculation and the scattering theory approximation to the elastic $M_a = 0$ limit. One can see that, closer to resonance, the discrepancy between the scattering theory and the self-consistent approach becomes more pronounced, whereas for weak electron–phonon coupling they almost coincide.

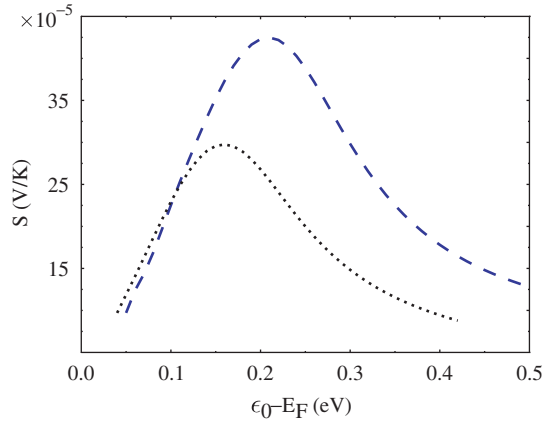

Figure 2. Seebeck coefficient versus energy position of the molecular level for the model of Equation (28). Shown are the results with (dashed line, blue) and without (dotted line, black) the electron–phonon interaction. The calculation was performed at $V = 0.05\,\mathrm{V}$. The other parameters are the same as in Figure 1.

In the following figures, we consider the inelastic effects only within the scattering theory approximation (which requires far less numerical effort). The dependence of S on the energy gap $\varepsilon_0 - E_F$ is shown in Figure 2, and its variation as a function of ω_0 is displayed in Figure 3. In these figures, V is kept at the value 0.05 V and all unvaried parameters are the same as in Figure 1. Finally, in Figure 4 we compare the self-consistent results (some of them already shown in Figure 1) obtained for different choices of electron–phonon coupling M_a and vibrational broadening Ω^{ph}.

The following observations can be made regarding these results.

1. In contrast to the inelastic tunneling features usually observed in the second derivative $\mathrm{d}^2I/\mathrm{d}V^2$ of the current–voltage characteristic near $|eV| = \hbar\omega_0$, no such threshold behaviour is seen in Figure 1. This lack of threshold behaviour in the inelastic contribution to the Seebeck coefficient results from the fact that thermoelectric conduction is associated with the tails of the lead Fermi–Dirac distributions, and these tails wash away any threshold structure.
2. Inelastic contributions can have a substantial effect on the Seebeck coefficient and its voltage dependence, however the assessment of these contributions is sensitive to the approximation used and cannot generally be based on the scattering theory level of calculation. Indeed, as seen in Figure 1 the behaviour of $S(V)$ may change qualitatively upon going from the scattering to the self-consistent calculation.

3. Focusing on the self-consistent results, Figures 1 and 4 show that the inelastic effect on the Seebeck coefficient can be positive or negative, depending on the other energetic parameters in the system. A change of sign as a function of ε_0 is seen also in the scattering theory results of Figure 2. The existence of a similar crossover in the self-consistent results can be inferred by comparing Figures 1(a) and (b).
4. A smaller value of the electron–phonon coupling M_a naturally leads to a smaller difference between the self-consistent and scattering theory calculations (compare Figures 1(a) and (c)). The coupling chosen in Figure 1(c) is still strong enough to result in an appreciable difference between the inelastic and elastic results.
5. In Figure 2, the Seebeck coefficient is seen to go through a maximum as a function of the gap $\varepsilon_0 - E_F$, with the inelastic contribution affecting the position and height of the observed peak. The behaviour seen in Figure 2 can be rationalised by noting that for, say, $T_L > T_R$, electrons with energies $E > E_F$ contribute most to the left-to-right current, whereas those with $E < E_F$ dominate the right-to-left current. This gives no thermoelectric current when $\varepsilon_0 = E_F$, hence as $\varepsilon_0 \to E_F$, one needs a higher temperature difference in order to compensate for the same bias. As a result, the Seebeck coefficient decreases at $\varepsilon_0 - E_F \to 0$. On the other hand, when $\varepsilon_0 - E_F \gg \Gamma, k_B T$ the two contributions cancel each other out, and hence the Seebeck coefficient decreases once more.
6. The dependence of S on ω_0 (Figure 3 demonstrates this within a scattering theory level calculation) is in line with the expectation that S should attain its classical limit as the vibration becomes more rigid.
7. We have found (not shown) that the effects on S of varying the electronic (Γ) or vibrational (Ω) width show a similar trend as varying the gap $\varepsilon_0 - E_F$ or the vibrational frequency ω_0, respectively.

5. Conclusion

We have studied the influence of molecular vibration (inelastic effects) on the Seebeck coefficient for molecular junction transport using a simple model of one molecular level (representing the participating molecular state) coupled to two contacts and to one molecular vibration. Two approaches to the model were considered: a simplified scattering model represented by Equation (28) and the full self-consistent approach described in Section 2. The simplified approach ignores the mutual influence of the electronic and vibrational subsystems. Note that the structure of the expression for the current (Equation (28)) is just the difference between two scattering fluxes (left-to-right minus right-to-left). The results of the simplified model calculation were

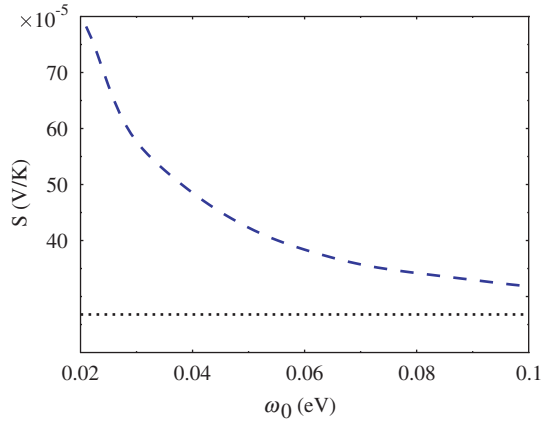

Figure 3. Seebeck coefficient versus vibrational mode frequency for the model of Equation (28). Shown are the result with (dashed line, blue) and without (dotted line, black) the electron–phonon interaction. The calculation was performed at $V = 0.05$ V. The other parameters are the same as in Figure 1.

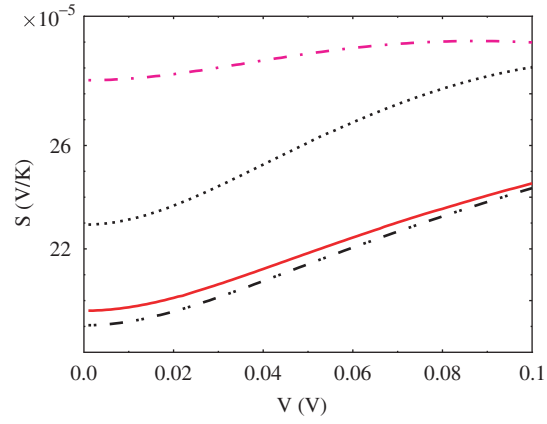

Figure 4. Seebeck coefficient versus applied bias for the model described in Section 2. The solid line (red) and the dash-dotted line (magenta) are identical to the solid lines (red) in Figures 1(a) and (c), respectively. Also shown are the results for $\Omega_L^{ph} = \Omega_R^{ph} = 0.002$ eV (dash-double dotted line, black). The elastic case (dotted line, black) is shown for comparison.

compared with the full self-consistent approach where both the mutual electron–vibration influence and vibration coupling to thermal baths are taken into account (for a detailed description of the approach, see the paper of Galperin *et al*. [29]). We show that inelastic effects have a non-negligible influence on the resulting Seebeck coefficient for the junction, for a reasonable choice of parameters. The electron–vibration interaction can either increase or decrease the Seebeck coefficient depending on the physical situation. We have studied the dependence of this influence on different parameters of the model (applied bias, the gap between the molecular level and the Fermi energy, the strengths of the coupling between the molecule and the contacts, between the tunneling electron and the molecular vibration, between the molecular vibration coupling and the thermal baths, and the frequency of the vibration). Comparing the results of the two approaches we show that the scattering-theory-based approach may fail both quantitatively and qualitatively. The experimental data presented by Reddy *et al*. [23] do not provide conclusive evidence for the relative importance of inelastic processes. More extensive measurements showing the dependence of the Seebeck coefficient on the junction parameters are needed in order to come to a definite conclusion. In particular, isotopic effects should influence the vibration-related part of the Seebeck coefficient (see Figures 3 and 4). A change in the electron–phonon coupling would also reveal the inelastic part of the Seebeck coefficient (see Figure 4). Finally, the results of our model calculations performed with a reasonable set of parameters show that the Seebeck coefficient is of the order of $\sim 10^{-4}\,\mathrm{V\,K^{-1}}$. The results reported by Reddy *et al*. [23] yield $S \sim 10^{-5}\,\mathrm{V\,K^{-1}}$. Since the molecules used in the experiment [23] are characterized by a relatively large gap $\varepsilon_0 - E_F$, our results are in good agreement with the measured data. Indeed, for $\varepsilon_0 - E_F \sim 1\,\mathrm{eV}$ the calculated Seebeck coefficient (see Figure 2) is of the same magnitude as the experimentally observed value.

Acknowledgements

M.G. and M.A.R. are grateful to the DARPA MoleApps program, to NSF-MRSEC, NSF-Chemistry, and the NASA-URETI programs for support. The research of A.N. is supported by the Israel Science Foundation, the US–Israel Binational Science Foundation, and the Germany–Israel Foundation. This paper is dedicated to Raphy Levine – a friend, colleague and a pioneer in our field.

References

[1] A. Nitzan and M.A. Ratner, Science **300**, 1384 (2003).
[2] M.A. Reed and T. Lee, editors, *Molecular Nanoelectronics* (American Scientific, Stevenson Ranch, CA, 2003).
[3] J.M. Tour, *Molecular Electronics: Commercial Insights, Chemistry, Devices, Architectures and Programming* (World Scientific, River Edge, NJ, 2003).
[4] G. Cuniberti, G. Fagas, and K. Richter, editors, *Introducing Molecular Electronics* (Springer, Berlin, 2005).
[5] K. Schwab, E.A. Henriksen, J.M. Worlock *et al*., Nature **404**, 974 (2000).
[6] P. Kim, L. Shi, A. Majumdar *et al*., Phys. Rev. Lett. **87**, 215502 (2001).
[7] L. Shi and A. Majumdar, J. Heat Transfer **124**, 329 (2002).
[8] D. Cahill, K. Goodson, and A. Majumdar, J. Heat Transfer **124**, 223 (2002).
[9] N. Agrait, C. Untiedt, G. Rubio-Bollinger *et al*., Phys. Rev. Lett. **88**, 216803 (2002).
[10] D. Cahill, W.K. Ford, K.E. Goodson *et al*., J. Appl. Phys. **93**, 793 (2003).
[11] M.J. Montgomery, T.N. Todorov, and A.P. Sutton, J. Phys.: Condens. Matter **14**, 5377 (2002).
[12] B.N.J. Persson and P. Avouris, Surf. Sci. **390**, 45 (1997).
[13] A.P. van Gelder, A.G.M. Jansen, and P. Wyder, Phys. Rev. B **22**, 1515 (1980).
[14] A. Cummings, M. Osman, D. Srivastava *et al*., Phys. Rev. B **70**, 115405 (2004).
[15] I. Paul and G. Kotliar, Phys. Rev. B **67**, 115131 (2003).
[16] D. Segal, A. Nitzan, and P. Hanggi, J. Chem. Phys. **119**, 6840 (2003).
[17] D. Segal and A. Nitzan, Phys. Rev. Lett. **94**, 034301 (2005).
[18] D. Segal and A. Nitzan, J. Chem. Phys. **122**, 194704 (2005).
[19] K.R. Patton and M.R. Geller, Phys. Rev. B **64**, 155320 (2001).
[20] Y.C. Chen, M. Zwolak, and M. Di Ventra, Nano Lett. **3**, 1691 (2003).
[21] M. Galperin, A. Nitzan, and M.A. Ratner, Phys. Rev. B **75**, 155312 (2007).
[22] J.C. Poller, R.M. Zimmermann, and E.C. Cox, Langmuir **11**, 2689 (1995).
[23] P. Reddy, S.-Y. Jang, R.A. Segalman *et al*., Science **315**, 1568 (2007).
[24] M. Galperin, M.A. Ratner, and A. Nitzan, J. Phys.: Condens. Matter **19**, 103201 (2007).
[25] M. Paulsson and S. Datta, Phys. Rev. B **67**, 241403(R) (2003).
[26] E. Macia, Nanotechnology **16**, S254 (2005).
[27] D. Segal, Phys. Rev. B **72**, 165426 (2005).
[28] K. Walczak, Physica B **392**, 173 (2007).
[29] M. Galperin, A. Nitzan, and M.A. Ratner, Phys. Rev. B **73**, 045314 (2006).
[30] B.J. LeRoy, S.G. Lemay, J. Kong *et al*., Nature **432**, 371 (2004).
[31] A. Mitra, I. Aleiner, and A.J. Millis, Phys. Rev. B **69**, 245302 (2004).

[32] G.D. Mahan, *Many-particle Physics*, 2nd ed. (Kluwer Academic/Plenum, New York, 2000).
[33] I.G. Lang and Yu.A. Firsov, Sov. Phys. JETP **16**, 1301 (1963).
[34] Y. Meir and N.S. Wingreen, Phys. Rev. Lett. **68**, 2512 (1992); A. Jauho, N.S. Wingreen and Y. Meir, Phys. Rev. B **50**, 5528 (1994).
[35] H. Haug and A.-P. Jauho, *Quantum Kinetics in Transport and Optics of Semiconductors* (Springer, Berlin, 1996).
[36] P.N. Butcher, J. Phys.: Condens. Matter **2**, 4869 (1990).
[37] L.D. Landau and E.M. Lifshitz, *Statistical Physics*, Part 1 (Pergamon Press, London, 1968).
[38] M. Abramowitz and I.A. Stegun, editors, *Handbook of Mathematical Functions with Formulas, Graphs, and Mathematical Tables* (Dover, New York, 1964).
[39] M. Galperin, M.A. Ratner, and A. Nitzan, J. Chem. Phys. **121**, 11965 (2004).